The Journal of Experimental Biology 202, 1589–1602 (1999)
Printed in Great Britain © The Company of Biologists Limited 1999
JEB1949

HEAT TRANSFER FROM STARLINGS *STURNUS VULGARIS* DURING FLIGHT

S. WARD[1], J. M. V. RAYNER[2], U. MÖLLER[3], D. M. JACKSON[1], W. NACHTIGALL[3] AND J. R. SPEAKMAN[1,*]

[1]*Aberdeen Centre for Energy Regulation and Obesity, Department of Zoology, University of Aberdeen, Tillydrone Avenue, Aberdeen AB24 2TZ, UK,* [2]*School of Biological Sciences, University of Bristol, Woodland Road, Bristol BS8 1UG, UK* and [3]*Institüt der Zoologie, Universität des Saarlandes, D-66041 Saarbrücken, Germany*

*e-mail: j.speakman@abdn.ac.uk

Accepted 25 March; published on WWW 20 May 1999

Summary

Infrared thermography was used to measure heat transfer by radiation and the surface temperature of starlings (*Sturnus vulgaris*) (*N*=4) flying in a wind tunnel at 6–14 m s^{-1} and at 15–25 °C. Heat transfer by forced convection was calculated from bird surface temperature and biophysical modelling of convective heat transfer coefficients. The legs, head and ventral brachial areas (under the wings) were the hottest parts of the bird (mean values 6.8, 6.0 and 5.3 °C, respectively, above air temperature). Thermal gradients between the bird surface and the air decreased at higher air temperatures or during slow flight. The legs were trailed in the air stream during slow flight and when air temperature was high; this could increase heat transfer from the legs from 1 to 12 % of heat transfer by convection, radiation and evaporation (overall heat loss). Overall heat loss at a flight speed of 10.2 m s^{-1} averaged 11.3 W, of which radiation accounted for 8 % and convection for 81 %. Convection from the ventral brachial areas was the most important route of heat transfer (19 % of overall heat loss). Of the overall heat loss, 55 % occurred by convection and radiation from the wings, although the primaries and secondaries were the coolest parts of the bird (2.2–2.5 °C above air temperature). Calculated heat transfer from flying starlings was most sensitive to accurate measurement of air temperature and convective heat transfer coefficients.

Key words: flight, thermoregulation, infrared thermography, bird, starling, *Sturnus vulgaris*.

Introduction

Most surfaces of birds are covered by feathers. These provide high levels of insulation in cold conditions, but the insulation could potentially lead to overheating during flight when metabolism rate typically rises to between 10 and 23 times the basal metabolic rate (Masman and Klassen, 1987; Rayner, 1990; Ward et al., 1998; Winter and von Helversen, 1998). The mechanical power for forward flapping flight is equivalent to only 10–20 % of metabolic power (Masman and Klassen, 1987; Biewener et al., 1992; Norberg et al., 1993; Chai and Dudley, 1995; Rayner, 1995; Dial et al., 1997). The remaining 80–90 % is converted to heat, largely as a by-product of the transformation of chemical to kinetic energy in the flight muscles (Hill, 1938). Increased heat production during flight must be offset by an increase in heat loss, particularly during prolonged flights when heat storage accounts for less than 1 % of the heat produced (Craig and Larochelle, 1991). Heat generated during flight could present a particular problem at high air temperature (T_a) in combination with heat gained from solar radiation (Bryant, 1983; Speakman et al., 1994).

The aerodynamic requirements for flight prevent some of the mechanisms that stationary birds can use to regulate heat loss such as raising or lowering the feathers or tucking the head under the wing. Flying birds can increase the surface area for heat dissipation by trailing the legs in the air stream (Baudinette et al., 1976; Torre-Bueno, 1976; Bryant, 1983; Biesel and Nachtigall, 1987) or can increase evaporative heat loss (q_{evap}) by opening the bill (Torre-Bueno, 1978; St-Laurent and Larochelle, 1994). Both these strategies have disadvantages since trailing the legs will increase drag, and hence the cost of flight, and high levels of q_{evap} could cause dehydration during long flights (Carmi et al., 1992; Klassen, 1995). Neither leg-trailing nor bill-opening is routinely used by passerine birds during flight at moderate T_a in the wild, so the capacity to dissipate heat from the rest of the body presumably increases by at least 10-fold between rest and flight. Part of the increase in heat transfer during flight will be accounted for by the greater surface area when the wings are opened, but the increase in surface area alone is not great enough to account for the change in heat loss.

Three sections of the body of a flying bird have been suggested to be particularly important for heat dissipation during flight: underneath the wings (Tucker, 1968; Baudinette et al., 1976; Biesel and Nachtigall, 1987; Craig and Larochelle, 1991), the legs (Steen and Steen, 1965; Martineau and Larochelle, 1988) and the head (St-Laurent and Larochelle, 1994). One might anticipate that the underside of the wings, and

especially the ventral brachial areas (see Fig. 1), would be most important because they have a large surface area, few feathers and could contribute to the difference in heat loss between perching and flying birds since they are not exposed when a bird is perching. Experiments in which pigeons (*Columba livia*) were submitted to heat stress demonstrated that the wings, legs and head can dissipate respectively 11 %, 50–65 % and 30–50 % of a heat load equivalent to that generated during flight (Martineau and Larochelle, 1988; Craig and Larochelle, 1991; St-Laurent and Larochelle, 1994). These experiments suggested that the wings were much less important for heat loss than was thought previously (Tucker, 1968), since 3–6 times more heat was lost through the legs and head.

Heat transfer theory predicts that the rate of heat loss by forced convection (q_{conv}) will be much greater than that by radiation (q_{rad}) at the speeds, bird surface temperatures (T_s) and T_a normally experienced by flying birds (Holman, 1986; Walsberg, 1988; Incropera and DeWitt, 1996). Calculation of q_{conv} requires knowledge of T_s and the convective heat transfer coefficient (h). The value of h can be predicted for simple geometric forms but must be determined experimentally to provide an accurate value for complex shapes such as animals (Gates, 1980; Holman, 1986; Incropera and DeWitt, 1996). The value of h has been measured from the cooling rate of gold-plated copper models of cylinders, arcs and cones that approximate the shapes of animal ears (Wathen et al., 1974). Heat transfer from these model appendages was close to that predicted for cylinders in cross flow at air speeds of 0.4–3.1 m s^{-1}, so q_{conv} for at least some animals can be approximated at slow wind speeds using values of h derived from simple shapes.

Calculation of q_{conv} and q_{rad} requires detailed knowledge of T_s. This information can be obtained from thermocouples attached to the surface of an animal. For example, 600 thermocouples were used to characterise the T_s of the tail of the coypu (*Myocastor coypus*) (Krattenmacher and Rübsamen, 1987). A different approach is required to measure T_s during flight, as large numbers of thermocouples would prevent an animal from flying. Infrared thermography allows detailed non-invasive measurement of T_s from the intensity of infrared radiation emitted by the animal (Speakman et al., 1997). Details of the physical principles that underlie thermography and a summary of its biological applications are given by Speakman and Ward (1998). This technique has been used previously to measure T_s of several birds and mammals at rest (Williams, 1990; Klir and Heath, 1992; Phillips and Sanborn 1994) and during flight (Lancaster et al., 1997).

We used infrared images of starlings flying in a wind tunnel to measure q_{rad} and to calculate T_s. Birds were flown in a wind tunnel to facilitate positioning the bird in the field of view of the thermal imager. Convective heat transfer was calculated from T_s and h. The value of h for a flying starling was predicted from those applicable to flat plates or cylinders, and was measured using a heated model bird. Air temperature and flight speed were varied to examine their effects on the ability of starlings to dissipate heat during flight since changes in air speed and temperature theoretically alter q_{conv} and q_{rad} as well as altering aerodynamic force production and therefore, presumably, internal heat generation.

Materials and methods

Wind tunnel

Starlings (*Sturnus vulgaris*) were flown in a closed-section variable-speed Göttingen-type wind tunnel at the University of Saarland, Saarbrücken, Germany (Biesel et al., 1985; Nachtigall, 1997). Birds were prevented from leaving the 1 m×1 m×1 m flight chamber upwind by wire mesh (25 mm hexagonal, 1 mm diameter) and downwind by vertical plastic chords (1 mm diameter, 1 cm apart). The top of the flight chamber was made of glass. The floor and walls of the chamber and the tunnel sections immediately up- and downwind of the flight section were constructed from wood. Thermal images were obtained through a hole (0.2 m×0.15 m) in one side wall of the flight chamber. The lens of the thermal imager was surrounded by transparent acetate film which blocked the rest of the hole to minimise disturbance of the air flow in the tunnel. The same side wall of the tunnel was replaced with a sheet of glass to allow lateral cine filming. Air speed was monitored downwind of the flight chamber with a pitot-static tube connected to a manometer. Air speed could be controlled to within ±0.2 m s^{-1} and was measured to ±0.1 m s^{-1}. Tunnel wall temperature (T_{wall}) was measured on the side wall opposite the thermal imager within the field of view of the thermal imager.

Birds and training

Starlings (seven hand-reared and eight wild-caught adult birds captured under licence from Scottish Natural Heritage in Aberdeenshire, UK) were housed in groups of 3–4 birds in approximately 2 m×2 m×2 m indoor cages and fed *ad libitum* on a mixture of moistened puppy pellets (Eukanuba), poultry pellets and cage bird egg food supplemented with mealworms and cage bird vitamin and mineral supplement. Birds were accustomed to the wind tunnel by placing them individually in the flight chamber, where they preferred to stand on a perch rather than the smooth floor of the chamber. Birds flew spontaneously when the perch was retracted into the floor of the chamber. The perch was returned after progressively longer periods of flight until the birds that had been trained successfully (N=4 wild-caught birds) would fly continuously for up to 1 h twice daily.

Bird surface area

Images of the surface of flying starlings were divided into 14 sections to allow assessment of regional T_s distribution and heat transfer (Fig. 1). The surface area of each section was calculated from dorsal and lateral cine film images of starlings in wind-tunnel flight taken simultaneously from near-perpendicular viewing angles (Photo-Sonics Series 2000, 16 mm 1Pl cameras; 255 frames s^{-1}; 16 mm Agfa XTR 250/XTS 400 colour negative film) (Möller, 1998). The surface areas of the flat projections of each section on the body were measured from three lateral cine film images. Dorsal and ventral brachial and maximum primary and secondary section

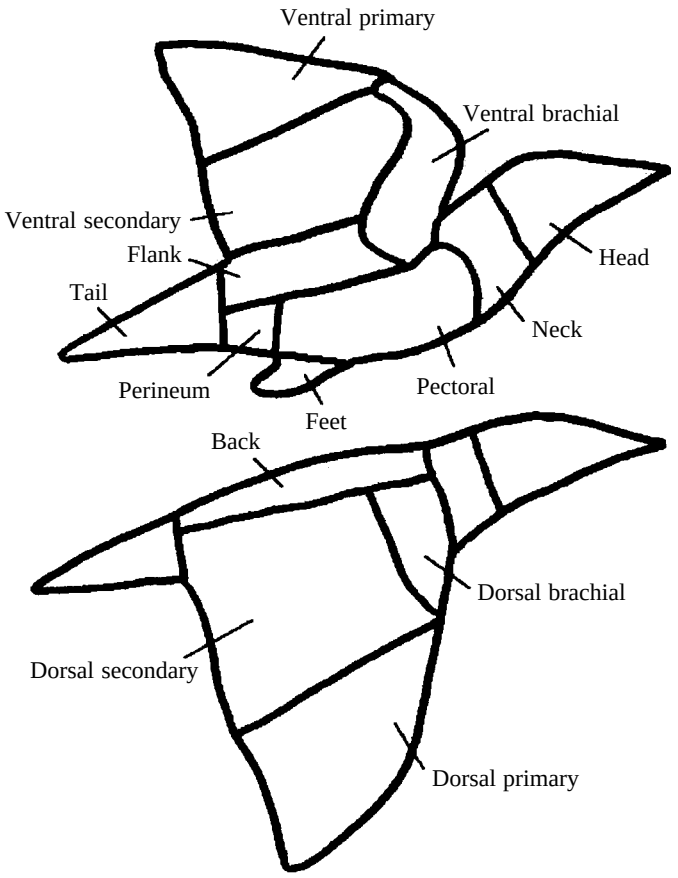

Fig. 1. The 14 sections of the surface of a flying starling.

areas were measured from three dorsal cine film images taken during flight at 10 m s^{-1} in which the wings were fully outstretched. Variation in the dimensions of the dorsal and ventral primary and secondary sections during the wingbeat cycle was quantified at each of 50 steps during five complete wing beats. The degree to which the wings were perpendicular to the dorsal camera at each of the steps was taken into account, since calculations were performed using the *x*, *y* and *z* coordinates of five points on the wing surface calculated from the simultaneous lateral and dorsal cine film images. These points were the tip of the secondary closest to the body (A), the tip of the secondary furthest from the body (B), the hand joint (C), the arm joint (D) and the wingtip (E). Variation in the surface area of the secondaries was calculated from the change in surface area of the rectangle ABCD. The area between these points was determined at each of the 50 steps during the wingbeat cycle from the scalar product of the absolute value of the diagonals AC and BD (*s*ACBD), the ratio of the absolute values of the diagonals (*abs*ACBD) and the angle (ϕ) between the diagonals, where $abs\text{ACBD}=\sqrt{(\text{AC})^2}/\sqrt{(\text{BD})^2}$, $s\text{ACBD}=\text{AC}\times\text{BD}$ and $\phi=\cos^{-1}(s\text{ACBD}/abs\text{ACBD})$. The area of the rectangle ACBD (A_{ABCD}) was calculated from: $A_{\text{ABCD}}=(abs\text{ACBD}/2)\sin\phi$. Fluctuations in the area of the primaries were calculated from changes in the area of the triangle BCE(A_{BCE}). The absolute lengths of the sides of the triangle were calculated as: $a=\sqrt{(\text{BC})^2}$, $b=\sqrt{(\text{BE})^2}$, $c=\sqrt{(\text{CE})^2}$. Half of the sum of the sides *S* was calculated from: $S=(a+b+c)/2$, and the area A_{BCE} was calculated from: $A_{\text{BCE}}=\sqrt{[S\times(S-a)\times(S-b)\times(S-c)]}$.

All surface areas were scaled to life size using the ratio of bird length (tip of bill to end of tail) in the image to actual bird length. Mean dimensions were used to calculate the surface areas of each section assuming that the head was a cone (with no base) and that the tail and ventral and dorsal primary, secondary and brachial sections were flat plates. The curvature of the head, neck, pectoral, perineum, flanks and back was taken into account when calculating the surface area of these sections from their flat projections. The mean surface area of the flank and the three sections under the wing was reduced by 1 % to take into account time spent with the wings folded against the body during bounds in flight at 10 m s^{-1} (Tobalske, 1995). The surface area of the legs was calculated assuming that they were a series of cylinders when the legs and feet were trailed in the air stream and that half the surface was exposed when the legs were tucked up against the body.

Bird surface temperature

The mean surface temperature (T_{s}) of each section of the body was calculated from q_{rad} in the 6–12 μm waveband (Speakman and Ward, 1998). Infrared radiation was detected by an Agema Infrared Systems Thermovision 880 system with a 20 ° lens linked to a dedicated thermal-imaging computer (TIC-8000) running CATS E 1.00 software. Bird surface temperature (±0.1 °C) was calculated by the software using T_{wall} measured to ±0.3 °C with a Digitron thermistor, assuming the emissivity of the bird to be 0.95 (Cossins and Bowler, 1987). Radiation was assumed to be exchanged only between the surface of the bird and the walls of the flight chamber, not between different parts of the bird's surface. Effects of viewing angle on q_{rad} were not included since only small parts of the edges of the images were viewed at angles of less than 10 ° (Sparrow and Cess, 1966; Clark, 1976).

Images of starlings were captured manually during flights when the bird flew in the field of view of the thermal imager; those in which the bird's wings were at maximum up- or downstroke were saved for analysis (N=2–4 per 30 min flight). The thermal imager was placed 0.6–0.7 m from the flying bird so that a complete image of the bird filled almost the whole field of view (Fig. 2). Each pixel in the image represented 1–3 mm^2 on the bird. The images analysed were obtained after 2–25 min of flight.

Variation in bird surface temperature with air temperature and wind speed

The mean T_{s} of each section of the body was measured by thermography during four flights by each bird at 10.2±0.3 m s^{-1} at air temperatures (T_{a}) between 15 and 25 °C to examine the effects of T_{a} upon T_{s}. Thermal images from eight flights by each bird at flight speeds between 6 and 14 m s^{-1} were collected to examine effects of flight speed on T_{s}. Since T_{a} in the tunnel could not be controlled, these data were examined in a multiple regression model that included

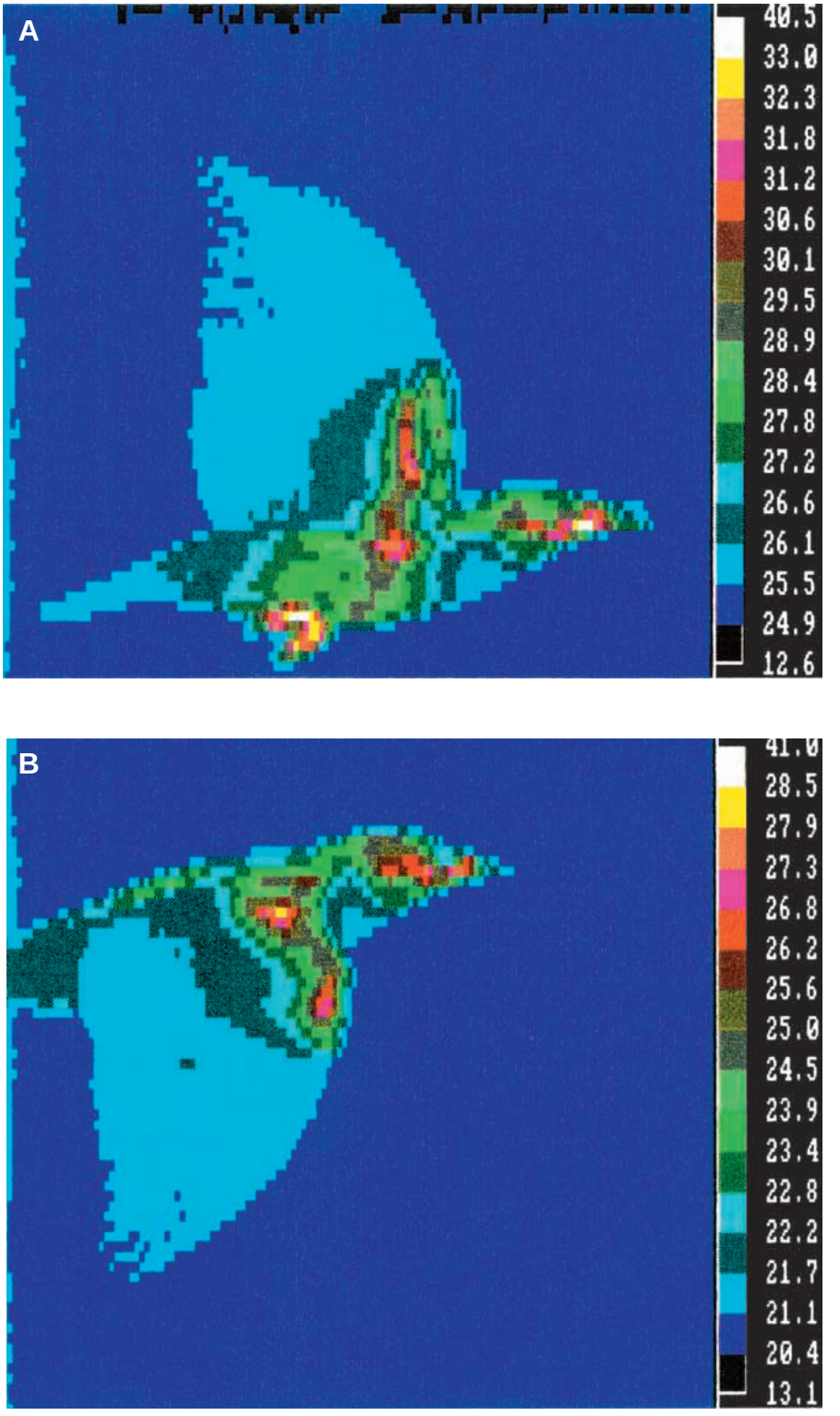

Fig. 2. Thermal image of a flying starling with the wing at (A) maximum upstroke (air temperature T_a=25.1 °C) and (B) maximum downstroke (T_a=20.5 °C). Colour levels represent temperature (°C) on a four-bit linear scale; the thermal-imaging system records temperature to eight-bit accuracy.

T_a, flight speed, individual bird and interactions between these variables. Regression models were repeated excluding the least important interaction or factor until all terms made a significant contribution (P<0.05) to variation in T_s. Cloacal temperature was measured 1–2 min before and after flight (Digitron thermistor, ±0.3 °C).

Heat transfer by radiation

The relationship:

$$q_{rad} = \sigma \times A \times \varepsilon_b \times \varepsilon_w (T_s{}^4 - T_{wall}{}^4), \quad (1)$$

was used to calculate heat transfer by radiation (q_{rad}, W) from each section of the body from mean surface temperature (T_s, K)

and surface area (A, m^2) of the section, where σ is the Stefan–Boltzmann constant ($5\times10^{-8}\,W\,m^{-2}\,K^{-4}$), ε_b is bird emissivity (assumed to be 0.95), ε_w is wall emissivity (assumed to be 1.0) and T_{wall} is chamber wall temperature (K) opposite where the bird flew measured using a thermistor (Holman, 1986).

Heat transfer by convection

The relationship:

$$q_{conv} = h \times A(T_s - T_a), \quad (2)$$

was used to calculate heat transfer by convection (q_{conv}, W) from each section of the body, where h is the convective heat transfer coefficient ($W\,m^{-2}\,°C^{-1}$) (Holman, 1986). T_a (°C) in the centre of the flight section was measured using a thermistor before and after each flight. Any change in T_a was assumed to be linear during flights. T_s (°C) was calculated from equation 1.

Values of h for rough, moving surfaces such as birds are unknown, so these were estimated as described in methods 1–3 below and were measured for a heated model bird (method 4) to examine the sensitivity of calculated q_{conv} to assumptions used in estimating h. The derivations of the equations used are explained by Holman (1986) and Incropera and DeWitt (1996).

Calculation of the heat transfer coefficient: method 1

The value of the heat transfer coefficient (h) was calculated for each section of the body assuming that conditions for convective heat transfer were the same as for laminar air flow over isolated flat plates of the same dimensions as the appropriate section of the body. For each section, the Reynolds number (Re) was determined from:

$$Re = u_{free} \times x/\nu, \quad (3)$$

where u_{free} is the air velocity ($m\,s^{-1}$) measured in the tunnel, x is the length (m) of the section of the body in the direction of air flow and ν is the kinematic viscosity of air ($15.69\times10^{-6}\,m^2\,s^{-1}$ at 300 K). Air speed over the sections of the body of the bird was assumed to be the same as u_{free}; the effects of the shape of the body and of air movements induced by the flapping wings were not included. Changes due to flapping were taken into account in the calculation of u_{free} past the wings. Wingbeat frequency, amplitude, upstroke ratio, upstroke sweep and stroke plane angle (Bilo, 1971; Tobalske and Dial, 1996) were determined from cine film images taken simultaneously from near-perpendicular viewing angles during flights at approximately $1\,m\,s^{-1}$ increments in speed between 6 and $14\,m\,s^{-1}$ (Möller, 1998). Wingbeat kinematics were used to calculate air speed past the wings by dividing the wing into 10 segments of equal width along the length of the wing and splitting the wingbeat cycle into 50 steps of equal duration. The value of Re was calculated for each segment during each time interval.

The mean Nusselt number (Nu) for each section was determined from:

$$Nu = 0.664 \times Re^{0.5} \times Pr^{0.333}, \quad (4)$$

where Pr is the dimensionless Prandtl number (0.708 for air at 300 K; Holman, 1986). The value of Nu was calculated for each of the 10 segments of the wing during each of the 50 steps in the wingbeat cycle. The mean value of h for each section of the surface of the bird was calculated from:

$$h = Nu \times k/x, \quad (5)$$

where k is the thermal conductivity of air ($0.02624\,W\,m^{-1}\,K^{-1}$ at 300 K; Holman, 1986). A mean value for h during the wingbeat cycle was calculated for each section on the wings.

Calculation of the heat transfer coefficient: method 2

Mean values of h are lower from long than from short plates because air flowing across plates has the greatest cooling effect near the leading edge and progressively less effect as it moves downwind owing to the build-up of the thermal boundary layer (Gates, 1980). Rather than treating each section of the surface of a starling as an isolated flat plate, as in method 1, values of h for the neck, legs, flanks, perineum, back, tail and dorsal and ventral secondary sections were modified to take into account the length of each section of the body upwind (Fig. 1). Values of q_{conv} from these sections were therefore lower when calculated using method 2 than using method 1. The approach described in method 1 was followed except that x was the combined length of the section in question (section 2) and the adjoining section upwind (section 1) in equations 3 and 5 when the mean values of Nu and h of sections 1 and 2 (h_{1+2}) were calculated. Convective heat loss from section 2 ($q_{conv,2}$) was calculated from:

$$q_{conv,2} = [(h_{1+2} \times l_{1+2}) - (h_1 \times l_1)]A_2\,(T_s - T_a), \quad (6)$$

where h_1 is the convective heat transfer coefficient for section 1 calculated using method 1, A_2 is the area of section 2, l_{1+2} is a dimensionless constant equal in value to the combined length of sections 1 and 2, and l_1 is a dimensionless constant equal in value to the length of section 1. Both sections were assumed to be at the mean temperature of section 2. The heat transfer coefficient for section 2 (h_2) was calculated by rearranging equation 2 to allow comparison between values of h for each section calculated using methods 1 and 2.

Calculation of the heat transfer coefficient: method 3

Calculation of h followed method 2 for all sections of the body except the legs. The value of h for the fully extended legs was estimated from the relationship applicable to cross flow over isolated cylinders. Tarsus and toe dimensions were measured from four starlings (tarsus length 2.5 cm, diameter 0.4 cm; toe length 1.2 cm, diameter 0.15 cm; S.D.<0.01 cm for all measurements). Computation of h for extended legs followed method 1, except that x is cylinder diameter in equations 3 and 5, and Nu was calculated from:

$$Nu = 0.683 \times Re^{0.466} \times Pr^{0.333}. \quad (7)$$

The value of h used to calculate q_{conv} from the legs depended upon how far the legs were extended in each image. Laminar flow with a thermal boundary layer (method 1) would be appropriate when the air flow across the tarsi was predominantly parallel to their long axis when the legs were held against the body. Cross flow (equation 7) would predominate when the legs

were fully extended. The extent to which the legs were exposed to the air stream during flight was measured in arbitrary units from the ratio of leg length (normal to the longitudinal body axis) to the width of the body to take into account differences in scale in thermal images taken when birds were different distances from the thermal imager. The value of h for the legs was assumed to vary linearly with the extent of leg exposure from the value calculated using method 1 when the legs were held against the body to that calculated using method 3 for fully extended legs. Variation in h with the extent of leg exposure reflected the change from laminar to cross flow over the legs as their exposure to the air stream was increased.

Calculation of heat transfer coefficient: method 4

We determined h empirically using a balsawood model of a flying starling that was heated on the surface of the wood using electricity running through high-resistance wire. The wood and wire were covered with leather to disperse the heat from the heating elements and to provide a surface of uniform emissivity that was similar to that of feathers. The wing of the model starling could be adjusted to maximum up- or downstroke. Thermal images of the heated model held in the wind tunnel at a wind speed of $10\,m\,s^{-1}$ were used to adjust the distribution of the heating elements and the electrical power supplied so that the T_s of the model was similar to that of a real bird. The value of h for the model was calculated from equation 2 using model surface area and mean T_s, assuming that 80 % of the electrical power supplied was lost by convection from the surface facing the thermal imager. It was assumed that 10 % was lost by radiation and 10 % by conduction to the interior of the model.

Statistical analyses

Values are presented as means ± S.D. Statistics were performed using Minitab (Ryan et al., 1985). The Bonferroni correction was used to adjust the 95 % confidence limit to P=0.0036 (0.05/14) for tests that were repeated for each of the 14 sections of the surface of starlings.

Results

Bird surface area

The mean surface area of a flying starling was 493±77 cm^2, to which the wings contributed 329±77 cm^2 (67 %) and the body and tail 164±5 cm^2 (Table 1). The surface area of a flying starling was 2.5 times greater than that predicted by the Meeh formula (for a 0.09 kg animal, $A=10\times M_b^{2/3}=201\,cm^2$, where M_b is body mass and A is the predicted surface area; Schmidt-Nielsen, 1984) since this formula does not include the area of the open wings. The Meeh formula is a good predictor of starling surface area when the wings are folded (Drent and Stonehouse, 1971).

Convective heat transfer coefficient

The values of h of each section of the body at a flight speed of 10.2±0.3 $m\,s^{-1}$ calculated using methods 1 and 2 are shown in Table 1. Thermal boundary layer thickness increases with distance along a surface from which heat is transferred, so long thin sections, such as the flanks and back, had lower values of h than sections such as those on the wings which were shorter in the direction of air flow. The value of h was greater for the wings than for the body because of the additional air speed past the wings caused by flapping. Method 2 predicted much lower values of h than method 1 for short sections such as the neck and perineum, which were downwind of other sections of the body. Values of h predicted by methods 1–3 varied with the square root of flight speed (equations 3–5). A mean value of h of 63±31 $W\,m^{-2}\,°C^{-1}$ (N=6) was predicted for an entire starling by method 4.

Table 1. *Surface area, the heat transfer coefficient* h *and the difference between surface temperature (*T_s*) and air temperature (*T_a*) for the 14 sections of the surface of four starlings flying at 10.2±0.3 m s* $^{-1}$ *and 22.8±0.1 °C*

	Surface area $\times 10^3$ (m^2)	Heat transfer coefficient, h ($W\,m^{-2}\,°C^{-1}$)		T_s–T_a (°C)
		Method 1	Method 2	
Legs	4.2±0.5	78	22	6.8±1.3
Ventral brachials	48.1±2.0	78	78	6.0±0.7
Head	14.7±0.2	65	65	5.3±0.6
Dorsal brachials	32.7±3.9	91	91	4.7±0.4
Pectoral	37.8±4.2	47	47	4.4±0.4
Flanks	33.0±4.4	53	25	3.8±0.4
Perineum	8.0±0.7	85	22	3.4±0.4
Neck	6.6±0.8	134	31	2.9±0.3
Back	38.7±2.4	45	24	2.8±0.8
Dorsal secondaries	57.4±18.6	50	29	2.5±0.4
Tail	17.5±1.8	52	21	2.5±0.9
Ventral secondaries	53.6±17.4	52	28	2.4±0.4
Dorsal primaries	71.3±24.7	54	51	2.2±0.5
Ventral primaries	65.7±22.8	56	52	2.2±0.4

Values are means ± S.D., N=4.

Surface areas for the primary and secondary sections refer to mean area during the wingbeat cycle. The surface area of the fully extended legs was $8.5\times10^{-3}\,m^2$. Heat transfer coefficients calculated by method 3 for the fully extended legs were 180 $W\,m^{-2}\,°C^{-1}$ for the tarsus and 261 $W\,m^{-2}\,°C^{-1}$ for the toes.

The value of h for an entire starling at $10\,m\,s^{-1}$ was 63 $W\,m^{-2}\,°C^{-1}$ when determined using method 4.

Air speed past the wings

Mean air speed across the wings was greater than that past the head because of the vertical and horizontal movements of the flapping wings that were additional to the flight speed. Air speed across the wings fluctuated during the wingbeat cycle because vertical movement of the wings was fastest during the middle of each stroke, and the wings moved backwards relative to the body during the downstroke and forwards during the

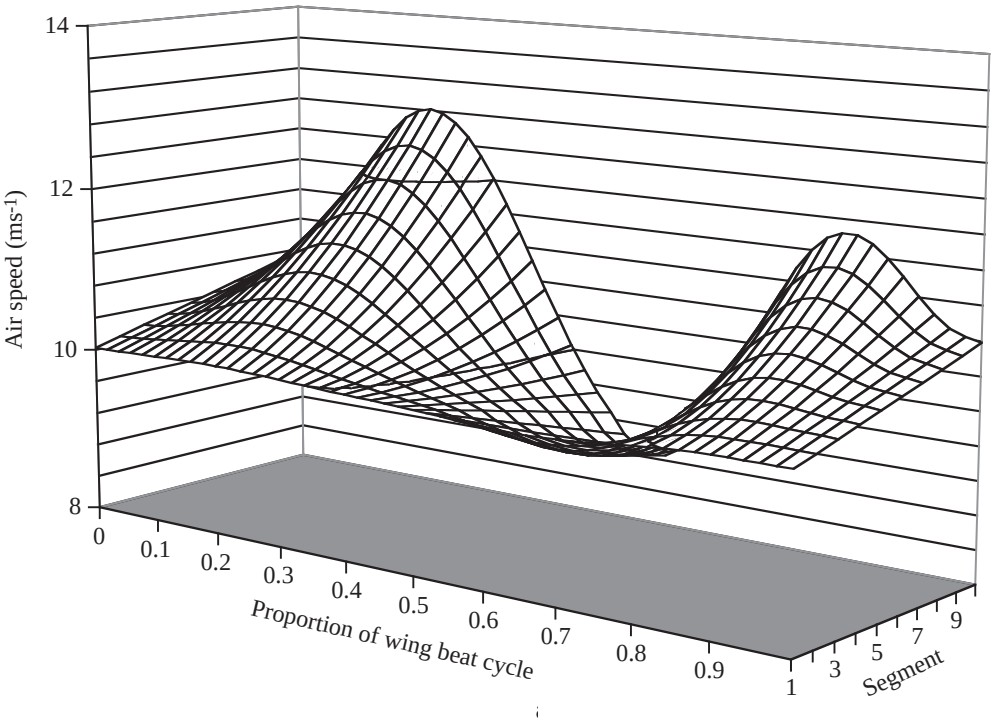

Fig. 3. Air speed past the wing of a starling flying at 10 m s^{-1}. Variation in the speed of each segment of the wing during the wingbeat cycle increased from the wing base (segment 1) to the wing tip (segment 10). The wingbeat cycle illustrated begins with the wing at the top of the upstroke. Kinematics measured by Möller (1998).

upstroke. Differences between flight speed and air speed past the wings, and fluctuations in wing speed during the wingbeat cycle, increased progressively towards the wing tip (Fig. 3). The wings moved most quickly relative to the body during slow flight. Mean air speed past the segment of the wing closest to the body was never more than 0.01 m s^{-1} greater than the flight speed. Fluctuations in air speed past this segment increased from ±0.07 m s^{-1} at a flight speed of 14.2 m s^{-1} to ±0.3 m s^{-1} at a flight speed of 6.1 m s^{-1}. Mean air speed across the wing tip segment was 2.2 m s^{-1} faster than flight speed at a flight speed of 6.1 m s^{-1}, declining to 0.7 m s^{-1} faster at a flight speed of 14.2 m s^{-1}. Fluctuations in air speed past the wing tip segment also increased from –0.8 to +1.8 m s^{-1} during flight at 14.2 m s^{-1} to –2.1 to +7.4 m s^{-1} during flight at 6.1 m s^{-1}.

Variation in bird surface temperature during flights

Both T_a and T_{wall} increased at 0.05±0.06 °C min^{-1} during flights (N=29). T_s of each of the 14 sections of the body of a flying starling increased with T_a during three 30 min flights for which images were obtained throughout the flight (regressions: P<0.05, N=12–38 images per body section, Fig. 4). The thermal gradient between T_a and T_s did not change with flight duration for any body section (regressions, P>0.2, N=12–38 images per body section). In further analyses, we have assumed that the duration of flight did not influence T_s. Thermal equilibrium at the body surface was reached more quickly than in the body core, which increases in temperature during flights of up to 60 min (Torre-Bueno, 1976; Aulie, 1971; Butler et al., 1977; Hirth et al., 1987).

Variation in bird surface temperature with air temperature

The T_s of all sections of the body increased with T_a during flight at 10.2±0.2 m s^{-1} (Table 2; Fig. 5A). The difference between T_s and T_a of the ventral brachials (Fig. 5B) and dorsal brachials (dorsal brachial T_s–T_a=(9.06±1.17)–(0.22±0.05)T_a, N=16, r^2=41 %, P<0.001, means ± S.D., temperature in °C) declined as T_a rose. The legs, ventral brachials and head were the hottest parts of flying starlings, with mean T_s values, respectively, 6.8, 6.0 and 5.3 °C greater than that of the air when T_a was 22.8±0.1 °C (Table 1). The coolest parts of the birds were the tail and the primary and secondary feathers, which were 2.2–2.5 °C warmer than the air.

Variation in bird surface temperature with flight speed

Multiple regression models were used to examine the effects

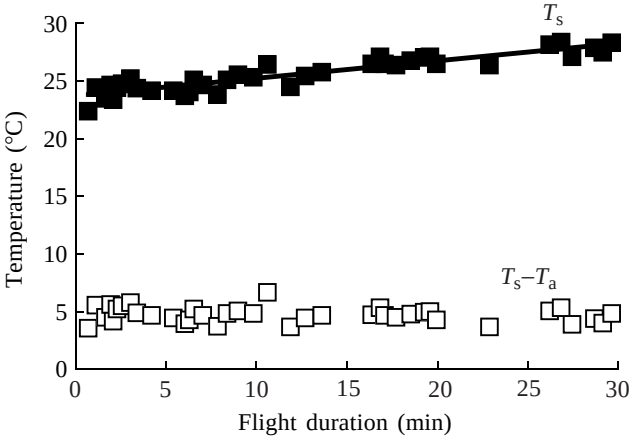

Fig. 4. Head surface temperature (T_s) (■) and the difference between head T_s and air temperature (T_a) (□) during a 30 min flight at 12.3 m s^{-1}. The solid line shows the regression: T_s =(23.7068±0.1729)t+(0.15169±0.0112), where t is time and regression variables are given as means ± S.D., r^2=84 %, P<0.001, N=36. The difference between head T_s and T_a did not vary with flight duration (P=0.3).

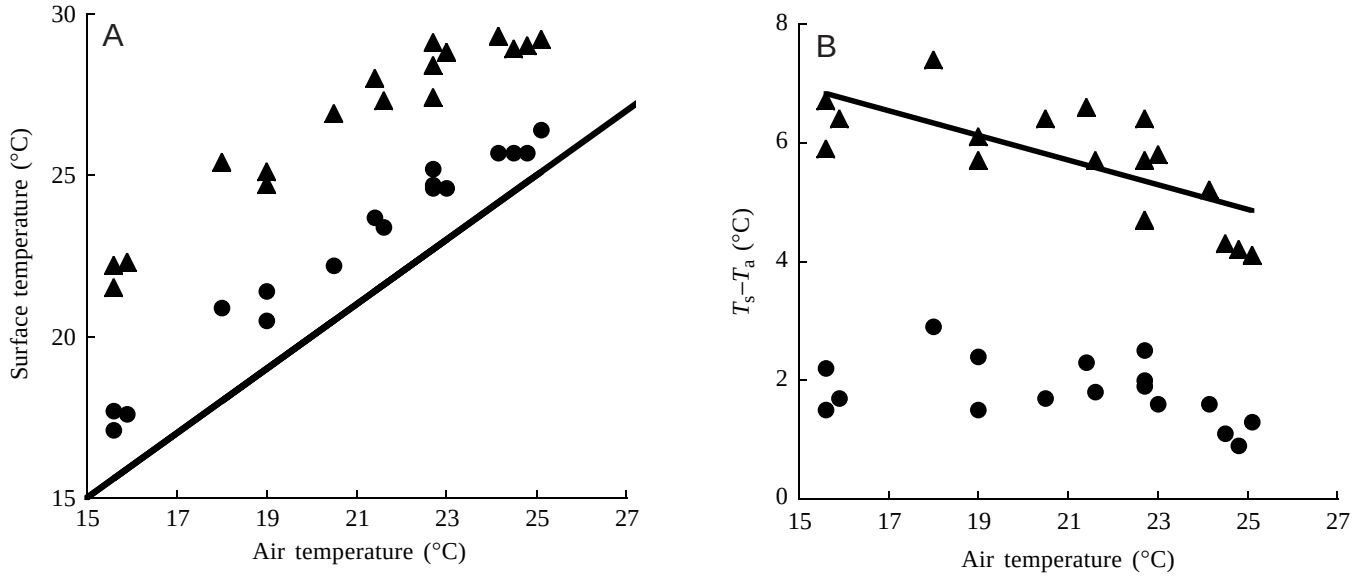

Fig. 5. (A) Surface temperature (T_s) of the ventral brachials (▲) and ventral primaries (●) of starlings flying at 10.2±0.2 m s^{-1} at a range of air temperature (T_a). The solid line shows T_s=T_a. Regression equations for the relationships between T_s and T_a are presented in Table 2. (B) Difference between T_s and T_a for the ventral brachials (▲) and ventral primaries (●) of starlings flying at 10.2±0.2 m s^{-1} at a range of T_a. The solid line shows the regression for the ventral brachials: T_s–T_a=(10.08±1.12)–(0.21±0.05)T_a, where the regression variables are given as means ± S.D., N=16, r^2=50 %, P<0.001. Ventral primary temperature did not vary with T_a (P=0.1).

of T_a, wind speed, individual bird and interactions between these factors upon T_s of each section (Table 3). The T_s of all sections increased with flight speed and T_a. The interaction between flight speed and T_a meant that the T_s of the legs, ventral brachials, head, pectoral, flanks, perineum, neck, back, tail and ventral secondaries declined as flight speed increased when T_a was greater than 21–23 °C. Inter-individual variation was not significant for any section. The T_a within the wind tunnel could not be controlled, so flights at different speeds were also performed at different T_a. When the effect of T_a upon T_s was removed by calculating the residuals from a regression of T_s against T_a, residual T_s increased with flight speed for the ventral brachials (Fig. 6), tail, primaries and secondaries.

Table 2. *Regression equations describing relationships between the surface temperature (T_s) (°C) of each section of the surface of a starling and air temperature (T_a) (°C) at flight speed 10.2±0.2 m s^{-1}*

	Intercept (°C)	Gradient	r^2 (%)
Legs	9.15±2.14	0.86±0.10	83
Ventral brachials	10.00±1.12	0.80±0.05	94
Head	8.83±1.40	0.81±0.06	91
Dorsal brachials	9.18±1.18	0.77±0.06	93
Pectoral	7.82±1.17	0.83±0.06	94
Flanks	6.66±1.04	0.85±0.05	95
Perineum	4.12±1.20	0.94±0.06	95
Neck	5.04±0.88	0.88±0.04	97
Back	4.75±1.08	0.90±0.05	95
Dorsal secondaries	3.42±0.94	0.92±0.04	97
Tail	3.42±1.15	0.94±0.06	95
Ventral secondaries	3.10±0.80	0.94±0.03	98
Dorsal primaries	3.42±0.94	0.92±0.04	97
Ventral primaries	3.69±0.67	0.92±0.03	98

N=16, P<0.001 for all regressions.
Values are means ± S.D., N=4.

Cloacal temperature

Cloacal temperature did not differ before and after flight

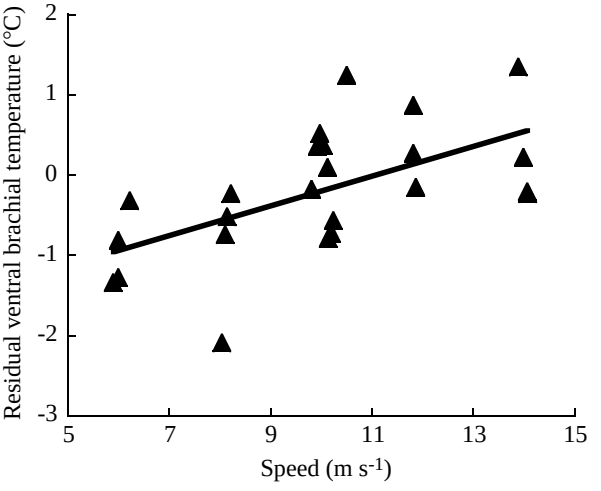

Fig. 6. Residual variation in ventral brachial surface temperature (T_s, °C) of starlings flying at a range of speeds (m s^{-1}) after the effects of air temperature (T_a) upon T_s had been taken into account. The solid line shows the regression: $T_{s,r}$=(–1.97±0.607)+(0.196±0.059)V, where V is speed and $T_{s,r}$ is residual brachial surface temperature, r^2=27 %, P=0.002, N=32. Regression variables are given as means ± S.D.

Table 3. *Regression equations describing the dependence of surface temperature (T_s) of each section of the surface of a starling upon air temperature (T_a), wind speed and the interaction between temperature and speed*

	Intercept	Air temperature (°C)	Speed ($m\,s^{-1}$)	Air temperature × speed	r^2 (%)
Legs	–36.1±14.3	3.03±0.71	4.23±1.43	–0.204±0.069	79
Ventral brachials	–7.2±6.7	1.52±0.33	1.65±0.67	–0.070±0.032	93
Head	–14.7±7.6	1.86±0.37	2.28±0.75	–0.102±0.037	91
Dorsal brachials	7.1±1.0	0.80±0.05	0.13±0.06		91
Pectoral	–9.2±6.4	1.61±0.31	1.64±0.63	–0.076±0.030	93
Flanks	–12.0±5.9	1.71±0.29	1.83±0.59	–0.084±0.029	94
Perineum	–11.2±7.2	1.68±0.35)	1.53±0.72	–0.074±0.35	93
Neck	–5.5±4.7	1.33±0.23	1.00±0.44	–0.042±0.023	97
Back	–8.8±5.9	1.52±0.29	1.28±0.59	–0.059±0.029	95
Dorsal secondaries	1.7±0.8	0.93±0.04	0.15±0.04		96
Tail	–11.1±5.9	1.54±0.29	1.42±0.59	–0.060±0.029	96
Ventral secondaries	–15.3±7.1	1.75±0.35	1.96±0.71	–0.086±0.034	93
Dorsal primaries	1.1±0.8	0.95±0.04	0.16±0.05		96
Ventral primaries	1.0±0.8	0.95±0.04	0.17±0.04		97

Missing values indicate that factors did not contribute significantly to regression models and regression equations quoted exclude those factors.

N=32, P<0.001 for all regressions.

Values are means ± S.D.

(mean value before flight 42.4±0.7 °C, after flight 42.2±0.8 °C; paired t-test: t=1.15, P=0.26, N=22 flights). Cloacal temperature after flight did not vary with flight speed or T_a (analysis of covariance, ANCOVA, P>0.4).

Behaviour during flight

The starlings were reluctant to fly in the wind tunnel for more than a few minutes when T_a was above 25 °C. Birds sometimes flew with their bills slightly open when T_a was less than 20 °C. Above this temperature, the bill was opened progressively wider as T_a increased. Both flight speed and T_a influenced the extent to which starlings exposed their legs to the air stream (Table 4). The legs were trailed in the air stream to a greater extent during slower flight and at higher T_a. Individual bird and interactions between bird, speed and T_a did not contribute significantly to regression models of the length of legs exposed to the air stream.

Heat transfer

The hottest parts of flying starlings had the greatest area-specific q_{rad} since the intensity of radiation emitted varies with the difference between T_s and T_{wall} (equation 1) (Tables 1, 5). The value of area-specific q_{conv} was determined by h as well as by the difference between T_s and T_a (equation 2). The value of h varied with the square root of flight speed (equations 3–5) and with location on the bird and differed amongst calculation methods 1–3 (Table 1). When h was calculated using method 2, q_{conv} was lower than when h was calculated using method

Table 4. *Multiple regression describing the effects of flight speed ($m\,s^{-1}$) and T_a (°C) on the length of legs exposed to the air stream*

	Coefficient	S.D.	t-ratio	P
Intercept	0.639	0.300	2.13	0.041
Temperature	0.032	0.014	2.24	0.033
Speed	–0.0838	0.016	–5.10	<0.001

N=32, P<0.001.

Table 5. *Values of the area-specific rate of heat loss by radiation (q_{rad}) and convection (q_{conv}) for each section of the surface of starlings during flight at 10.2±0.3 $m\,s^{-1}$ and 22.8±0.1 °C (N=4 birds)*

	Area specific q_{rad} ($W\,m^{-2}$)	Area specific q_{conv} ($W\,m^{-2}$)	
		Method 1	Method 2
Legs	38.4±7.6	523.5±99.4	145.6±27.6
Ventral brachials	32.4±4.2	440.7±55.0	440.7±55.0
Head	29.0±3.4	335.6±37.7	335.6±37.7
Dorsal brachials	25.8±2.5	411.8±38.9	411.8±38.9
Pectoral	24.2±2.4	201.8±19.3	201.8±19.3
Flanks	21.0±2.4	197.9±21.7	92.8±10.2
Perineum	18.7±2.4	262.7±3.0	67.5±0.8
Neck	15.8±1.8	398.6±67.4	91.6±15.5
Back	15.4±4.7	125.5±37.9	65.5±19.8
Dorsal secondaries	13.7±2.1	121.2±18.8	76.8±11.4
Tail	13.6±4.9	125.9±43.6	50.2±17.4
Ventral secondaries	12.5±2.2	115.7±20.1	66.4±11.1
Dorsal primaries	11.6±2.7	110.7±25.9	104.6±24.5
Ventral primaries	11.3±2.1	112.0±20.9	104.0±19.5

Methods 1 and 2 refer to the methods by which the heat transfer coefficient h was calculated.

Values are means ± S.D.

Table 6. *Absolute values of the rate of heat loss by radiation (q_{rad}) and convection (q_{conv}) for each section of starlings during flight at 10.2±0.3 m s^{-1} and 22.8±0.1 °C (*N=4 birds) and percentage contributions to dry and overall heat loss*

			q_{conv}					
	q_{rad}		Method 1		Method 2		Method 3	
	(W)	(%)[1]	(W)	(%)[2]	(W)	(%)[2]	(W)	(%)[2]
Legs	0.02±0.01	0.2	0.22±0.04	2	0.06±0.01	1	1.40±0.27	14
		0.1		*2*		*1*		*12*
Ventral brachials	0.16±0.02	1.6	2.10±0.26	20	2.12±0.26	25	2.12±0.26	21
		1.4		*18*		*21*		*19*
Head	0.04±0.01	0.4	0.49±0.06	5	0.49±0.06	6	0.49±0.06	5
		0.4		*4*		*5*		*4*
Dorsal brachials	0.08±0.01	0.8	1.35±0.13	13	1.35±0.13	16	1.35±0.13	13
		0.7		*11*		*14*		*12*
Pectoral	0.09±0.01	0.9	0.76±0.07	7	0.76±0.07	9	0.76±0.07	8
		0.8		*6*		*8*		*7*
Flanks	0.07±0.01	0.7	0.65±0.07	6	0.31±0.03	4	0.31±0.03	3
		0.6		*6*		*3*		*3*
Perineum	0.01±0.01	0.1	0.21±0.01	2	0.05±0.01	1	0.05±0.01	1
		0.1		*2*		*1*		*<1*
Neck	0.01±0.01	0.1	0.26±0.04	3	0.06±0.01	1	0.06±0.01	1
		0.1		*2*		*1*		*1*
Back	0.06±0.01	0.6	0.49±0.15	5	0.25±0.08	3	0.25±0.08	3
		0.5		*4*		*3*		*2*
Dorsal secondaries	0.08±0.01	0.8	0.70±0.11	7	0.44±0.07	5	0.44±0.07	4
		0.7		*6*		*6*		*4*
Tail	0.02±0.01	0.2	0.22±0.08	2	0.09±0.03	1	0.09±0.03	1
		0.2		*2*		*1*		*1*
Ventral secondaries	0.07±0.01	0.7	0.63±0.11	6	0.36±0.06	4	0.36±0.06	4
		0.6		*5*		*4*		*3*
Dorsal primaries	0.08±0.02	0.8	0.80±0.19	8	0.75±0.17	9	0.75±0.17	7
		0.7		*7*		*7*		*7*
Ventral primaries	0.07±0.01	0.7	0.73±0.14	7	0.68±0.13	8	0.68±0.13	7
		0.7		*6*		*7*		*6*
Total	0.9	9	9.6	92	7.8	90	9.1	91
		8		*82*		*79*		*81*

[1]Calculated from $q_{rad}/(q_{rad} + q_{conv})$, where q_{conv} was calculated using method 3.

[2]Calculated from $q_{conv}/(q_{rad} + q_{conv})$, where q_{conv} was calculated using the method at the head of the column.

Methods 1 to 4 refer to the methods by which the heat transfer coefficient h was calculated.

Values are means ± S.D.

Percentages in italics show contribution to overall heat loss ($q_{conv} + q_{rad} + q_{conv}$) where evaporative heat loss q_{evap}=1.3 W (calculated from Torre-Bueno, 1978).

Predicted q_{conv} was 10.5 W when h was calculated using method 4.

1 for all sections that were downwind of other parts of the body, since calculation using method 2 reduced the value of h for these sections (Table 5). Calculation of h using method 3 increased area-specific q_{conv} from the legs to 1481±281 W m^{-2} (compared with 146–524 W m^{-2} when h was calculated using methods 1 and 2; Table 5).

Absolute q_{rad} and q_{conv} from each section of the bird depended upon the surface area of the section as well the area-specific heat transfer rate. When h was calculated using methods 1 or 2, q_{conv} was 2–25 times greater than q_{rad} (Table 6). When h was calculated using method 3, q_{conv} was 4–16 times greater than q_{rad} for all sections other than the legs. For the fully extended legs, q_{conv} was 87 times greater than q_{rad}. Overall, q_{rad} accounted for 9% of dry heat loss (q_{conv}+q_{rad}) when q_{conv} was calculated using method 3. Sections that had high rates of q_{conv} per unit area or large surface areas were the most important routes of convective heat loss. Convection from the ventral brachials was the most important route of heat transfer from flying starlings. The ventral brachials accounted for 21% of dry heat loss when q_{conv} was calculated using method 3 because of the large surface area (Table 1) and high area-specific q_{conv} (Table 5) of this section. The dorsal brachials (13% of dry heat loss when q_{conv}

was calculated using method 3) were also important for convective heat loss. Convective heat loss from the legs could be varied from 0.06 W (1 % of dry heat loss, method 2) when they were folded against the body to 1.4 W (14 % of dry heat loss, method 3) when the legs were trailed in the air stream. Evaporative heat loss (q_{evap}) was not measured during the current study. This was calculated from bird mass and the relationship between evaporative water loss and T_a determined for starlings by Torre-Bueno (1978) (a third-order polynomial increase from 0.8 W at 15 °C to 1.6 W at 25 °C). Overall heat transfer during flight at 10.2 m s^{-1} and 22.8 °C was 11.3 W (9.1 W q_{conv} calculated by method 3+0.9 W q_{rad}+1.3 W q_{evap}, Table 6).

A sensitivity analysis showed that the overall heat transfer rate predicted for a flying starling changed by less than 0.1 W (1 %) if flight speed was altered by 0.2 m s^{-1}. We did not take into account variations in local air speed past some parts of the body due to the effect of the flapping wings, but these would also have a small effect on overall heat transfer unless large areas of the bird experienced local air speeds which differed greatly from those we used since h varies with the square root of air speed. Overall heat transfer changed by less than 0.1 W (1 %) if any of the variables that described wingbeat kinematics was changed by 10 %. The same error occurred if the surface area of any of the sections of the bird was altered by 1 cm^2 or if T_{wall} was altered by 0.3 °C. An alteration of 0.3 °C in dorsal or ventral brachial, primary or secondary T_s led to a change in heat loss of 0.1–0.2 W. Flight speed, wingbeat kinematics, T_s and surface areas were measured to a greater accuracy than the changes simulated in the sensitivity analysis. Calculated heat transfer was more sensitive to measurement error in T_a. A 0.3 °C change in T_a led to a 0.69 W (6 %) change in overall heat transfer from a flying starling, of which 0.67 W was due to changes in q_{conv} and 0.02 W to alteration in q_{evap} predicted from Torre-Bueno (1978). The thermistor used to measure T_a and T_{wall} was accurate to within 0.3 °C. The assumptions used to calculate the value of h had the greatest influence on overall heat loss since 81 % of overall heat loss occurred by convection and q_{conv} depended upon h.

The value of h measured using method 4 for the heated model bird at a wind speed of 10 m s^{-1} was 63 W m^{-2} °C^{-1}. Together with the mean T_s of starlings flying at that speed (2.8 °C), this predicted a q_{conv} of 10.5 W (equation 2). Closest agreement with q_{conv} calculated using method 4 was obtained when h was calculated using method 1 (q_{conv}=9.6 W; Table 6), but this was due to two simplifying assumptions that led to cancelling errors when q_{conv} was calculated using method 1 rather than because method 1 was the best way in which to calculate q_{conv}. The value of h from sections of the body that were downwind of other sections was overestimated when q_{conv} was calculated using method 1 since these sections were treated as isolated plates, which have greater values of h than parts of continuous surfaces. Calculation of h using method 2 removed this error, reducing q_{conv} to 7.8 W (Table 6). Overestimation of q_{conv} from the body was balanced by underestimation of heat transfer from the legs using method 1, since the legs were treated as flat plates held against the body. Convective heat transfer from the legs was underestimated by method 2 for the same reason. Method 3 used the more realistic analogy to cylinders in cross flow to calculate h for the legs when they were trailed in the air stream. A convective heat loss was 9.1 W when calculated using method 3. This differed by 1.4 W (13 %) from the value determined using method 4.

Discussion

The head and legs were the most important sections of the body for the regulation of heat transfer from flying starlings since bill-opening (and hence q_{evap}) and the amount of leg exposed to the air (and therefore q_{conv}) can be varied. Trailing the legs in the air stream would appear to be aerodynamically disadvantageous, since they would increase drag. However, since starlings fly at 10–12 m s^{-1} in the wild (S. Ward, unpublished data), they may need to increase drag using the legs as well as change their wingbeat kinematics to achieve stable flight at speeds as low as 6 m s^{-1} (Tobalske, 1995; Tobalske and Dial, 1996; Möller et al., 1997). The tail can be used to increase drag during slow and hovering flight (Thomas, 1996a,b), although the tail can usually provide lift whereas the legs provide only drag. Trailing the legs in the air stream by starlings and other passerines could therefore serve dual thermoregulatory and aerodynamic functions in slow flight, whilst in fast flight this would be beneficial only for thermoregulation. Birds such as waders, herons and storks that obligatorily trail their legs in the air stream behind their bodies when in flight regulate heat transfer from the legs using a rete system (Kahl, 1963) or by altering the flow of blood to the legs.

Starlings responded to increased T_a by progressively opening their bill during flight; this increases q_{evap} (St-Laurent and Larochelle, 1994). Starlings in the present study were reluctant to perform prolonged flights at T_a above 25 °C. This response to high T_a was similar to that reported in other studies of bird flight in wind tunnels. Starlings (Torre-Bueno, 1976), pigeons (Biesel and Nachtigall, 1987) and budgerigars (*Melopsittacus undulatus*) (Tucker, 1968; Byman et al., 1985) sometimes began to open their bills during wind-tunnel flight at T_a as low as 10 °C. In these studies, gape size gradually increased with T_a, until the bill was fully open at T_a between 28 and 30 °C. Starlings, pigeons and budgerigars trailed their entire legs in the air stream during flight at T_a between 27 and 36 °C and were reluctant to fly when T_a was above 28–37 °C (the present study; Torre-Bueno, 1976; Tucker, 1968; Byman et al., 1985; Biesel and Nachtigall, 1987). Leg-trailing during flight at high T_a has also been observed in 17 passerine and non-passerine species in the wild (Bryant, 1983). Overheating during flight at high T_a might potentially present a problem which could restrict the geographical range of well-insulated species. Starlings, however, are abundant in regions such as the southern United States (Price et al., 1995) in which T_a is often greater than the 25 °C at which they were reluctant to perform prolonged flight in our wind tunnel. Starlings are possibly more prone to heat stress during wind-tunnel flight than they are in the wild. This could be because wind tunnel-flight is more

thermally stressful, although a mechanism for this is unknown, or because flights by free-living starlings in hot climates are shorter than those required in wind tunnels. Most flights made by free-living adult starlings lasted less than 20 s during the nestling rearing period in Aberdeenshire (57 °N, T_a=12.5 during observations; S.D.=3.0, N=26 birds; S. Ward, personal observation). Therefore, although starlings do apparently make longer flights to reach communal roosts, flight duration can be surprisingly short during a 'demanding', period such as rearing nestlings, when nests are built close to suitable foraging sites.

Most of the mechanical work during flight occurs in the pectoral muscles (Biewener et al., 1992; Dial et al., 1997). The low conversion efficiency between chemical and mechanical work by muscle (Hill, 1938) means that substantial amounts of heat must also be produced in the pectoral muscles. This heat could potentially be dissipated directly from the breast; however, our thermal images showed that this was not the case (Fig. 2; Table 1). Starling skin temperature on the breast was within a few degrees of body core temperature (Torre-Bueno, 1976), so the insulation provided by the feathers immediately superficial to the pectoral section probably prevented the heat generated by the muscles from reaching the surface. Instead, heat was apparently transported to sections with few or no insulating feathers such as the legs, ventral brachials and head. These sections could be regarded as 'thermal windows' analogous to the ears of jackrabbits (*Lepus californicus*) (Hill and Veghte, 1976), elephants (*Elaphus maximus* and *Loxodonta africana*) (Williams, 1990) and foxes (*Vulpes* sp.) (Klir and Heath, 1992) or the tail of coypu (*Myocastor coypus*) (Krattenmacher and Rübsamen, 1987). The beak, legs and neck of ostrich (*Struthio camelus*). emu (*Dromaius novaehollandiae*) and double-wattled cassowary (*Casuarius casuarius*) (Phillips and Sanborn, 1994), the legs of storks (*Mycteria americana*) (Kahl, 1963) and the heads of chickadees (*Parus atricapillus*) (Hill et al., 1980), turkeys (*Meleagris gallopavo*) (Buchholz, 1996) and owls (*Tyto alba*) (McCafferty et al., 1998) have also been identified as important sites for heat loss in resting birds.

The ventral brachials were the most important sites of heat loss from flying starlings. Although this section represented only 10 % of the surface area of a flying starling, it accounted for 21 % of dry heat loss (19 % of overall heat loss). Convective heat loss from the ventral brachials was high because of their high T_s and h. Heat transfer from the six wing sections made up 62 % of dry heat loss and 55 % of overall heat loss. The large surface area of the primary and secondary feathers and their relatively high air speed meant that these sections dissipated 23 % of overall heat loss despite being among the coolest parts of the bird. Lancaster et al. (1997) found that, although the wings of Egyptian fruit bats (*Rousettus aegyptiacus*) were substantially cooler than the body, their large surface area meant that the wings accounted for 60 % of q_{conv} during flight.

Starling wings appeared to be much more important for heat transfer than the wings of pigeons since pigeon wings lost the equivalent of only 11 % of the heat generated during flight (Craig and Larochelle, 1991). Heat loss from pigeon wings may be lower than from the wings of starling because of the denser feathers under the wing (Aulie, 1971). Three differences in experimental procedure may also contribute to the difference between species. Contact with the air was not possible from the most proximal part of pigeon wings (equivalent to approximately 17 % of the ventral brachial section of starlings), and the increase in q_{conv} due to flapping the wings was not included since the pigeon wings were held static. Both these factors would tend to reduce the heat transfer capacity of pigeon wings. In addition, the source of the heat was from heat pads placed against the surface of the pigeons but mainly from the pectoral muscles of the starlings, potentially changing the relative importance of different parts of the body for heat loss.

We made three assumptions in measuring q_{rad} and T_s that potentially limited the accuracy of our measurements of heat transfer. First, we assumed that bird emissivity was 0.95. Starling emissivity has been measured as 0.85 (Porter and Gates, 1969) but, since emissivity changes with wavelength (Gubareff et al., 1960; Holman, 1986), we did not use this value because this was the average emissivity across an unknown waveband. Chickadee feather emissivity in the waveband in which we measured infrared radiation (6–12 μm) averaged 0.95, although it declined to 0.86–0.88 in the 1.9–5.8 μm waveband (Hill et al., 1980). The infrared emissivity of human skin is approximately 0.98 (Steketee, 1973), and Cossins and Bowler (1987) give values in the range 0.95–0.97 for biological materials. If the assumed emissivity of 0.95 differed by 0.05 from the true value, q_{rad} would change by 5 %, which would make a trivial contribution (less than 1 %) to overall heat transfer (Table 6). A change of 0.05 in emissivity would also alter T_s by 0.03 °C, leading to a change of 0.07 W in q_{conv}, which is less than 1 % of overall heat transfer. Deviation of actual emissivity from our assumption therefore led to minor changes in calculated heat transfer rates.

Our second assumption was that q_{rad} was not affected by viewing angle. Viewing angle was unlikely to affect q_{rad} across a wide range of angles since rough surfaces such as feathers produce diffuse radiation (Holman, 1986). However q_{rad} declines as surfaces are viewed at increasingly acute angles, particularly at angles less than 10 ° (Clark, 1976; Gubareff et al., 1960). The very edges of the head, pectoral, back and tail sections of starlings were viewed at such angles. Viewing angle also changes the surface area that is represented by each pixel on a thermal image: parts that are viewed at acute angles contribute fewer pixels to the image than parts that face directly towards the thermal imager. The magnitude of the effect of viewing angle upon q_{rad} was assessed for the pectoral section, assuming that it was a rectangle three times as long as it was wide, and that the surface equivalent to one pixel along one edge of the image was viewed at an angle of less than 10 °. The line of pixels along this edge would represent 9 % of the surface area of the pectoral section when starlings flew 0.6–0.7 m from the thermal imager. These pixels would appear to emit 50 % of the radiation that would have been detected if the thermal imager had viewed them normal to the surface if they were viewed at 5–10 ° (Clark, 1976). A reduction of 50 % in the q_{rad} of 9 % of the pectoral section would lead to a 4.5 %

underestimate in pectoral q_{rad}. A reduction of 4.5 % in radiation from each of the head, pectoral, back and tail sections would be equivalent to a total reduction in q_{rad} of 1.3 % (0.01 W), which was a 0.1 % change in overall heat transfer. Apparent T_s would change by less than 0.03 °C for these sections, changing q_{conv} from these sections by 1 % and overall q_{conv} by 0.1 %. The effects of viewing angle at the edges of the images therefore had trivial effects upon calculated heat transfer.

The third assumption in the calculation of q_{rad} was that the sections exchanged radiation only with the walls of the flight chamber and not with each other. Convex sections of the bird would only exchange radiation with the chamber walls, but the dorsal and ventral surfaces of the wings would 'see' each other when the wings were raised or lowered, and the ventral brachials would 'see' the flanks during the downstroke. Radiative exchanges with the rest of the bird rather than the chamber walls may reduce q_{rad} from the wings by 8 % (0.04 W) if q_{rad} is reduced by 50 % from 30 % of the wing surface for 50 % of the wingbeat. The thermal images that were analysed were taken when sections of the body faced towards the thermal imager rather than towards each other. Since q_{conv} was much greater than q_{rad}, any transient heating of the bird surface due to exchange of radiation with other parts of the body was assumed to have been dissipated by convection before the thermal image was taken. The thermal images showed the T_s that applied for 92 % of the time, so that any changes in q_{conv} due to transient changes in T_s would lead to negligible changes in overall heat transfer.

Infrared thermography allows non-invasive characterisation of the T_s and q_{rad} of active animals. These are measurements that would not be possible using methods that require physical contact. Calculations of heat transfer based on these data were not sensitive to current levels of accuracy of the thermal-imaging equipment or to the assumptions used to calculate T_s or q_{rad} of a three-dimensional, moving surface from a two-dimensional thermal image. Correct quantification of q_{conv} was important for accurate prediction of overall heat loss during flight, since 81 % of overall heat transfer occurred by forced convection. Infrared thermography provided measurements of T_s, but this was only one of the measurements needed to calculate q_{conv}. Accurate measurement of T_a and h and estimates of local airflow patterns based on detailed measurements of wingbeat kinematics were also necessary. Our estimates of q_{conv} were most sensitive to potential errors in determination of h although, encouragingly, values of h extrapolated from flat plates and cylinders gave results that were close to empirical determinations using a heated model. Future work to improve the accuracy of this approach should concentrate on accurate measurement of T_a and more refined determination of h for complex flapping shapes, including more detailed empirical modelling of heat transfer from the legs. Questions that might be addressed by using thermography include how birds vary T_s to conserve heat in cold conditions and how heat is dissipated in circumstances in which overheating is a potential problem. Heat transfer analysis might also be used as an alternative method by which to calculate energy expenditure during flight.

We thank Dietrich Bilo for help with the cine filming, Imke Breves and Michael Stephan for looking after the birds, Peter Anthony, Michael Glander and Wyn Pattullo for technical assistance, EPSRC for the loan of the Agema 880 thermal-imaging system and Douglas R. Warrick and an anonymous referee for suggesting improvements to an earlier draft of the manuscript. This work was supported by BBSRC grant GR/J36150 to J.R.S. and J.M.V.R. and British Council grant 680 to J.R.S., S.W. and W.N.

References

Aulie, A. (1971). Body temperatures in pigeons and budgerigars during sustained flight. *Comp. Biochem. Physiol.* **39**A, 173–176.

Baudinette, R. V., Loverage, J. P., Wilson, K. J., Mills, C. D. and Schmidt-Nielsen, K. (1976). Heat loss from feet of herring gulls at rest and during flight. *Am. J. Physiol.* **230**, 920–924.

Biesel, W., Butz, H. and Nachtigall, W. (1985). Einsatz spezieller Verfahren der Windkanaltechnik zur Untersuchung des freien Gleitflugs von Vögeln. In *BIONA Report 3* (ed. W. Nachtigall), pp. 109–122. Stuttgart: Gustav Fischer Verlag.

Biesel, W. and Nachtigall, W. (1987). Pigeon flight in a wind tunnel. IV. Thermoregulation and water homeostasis. *J. Comp. Physiol.* B **157**, 117–128.

Biewener, A. A., Dial, K. P. and Goslow, G. E. (1992). Pectoralis muscle force and power output during flight in the starling. *J. Exp. Biol.* **164**, 1–18.

Bilo, D. (1971). Flugbiophysik von Kleinvögeln. I. Kinematik und Aerodynamik des Flügelabschlges beim Haussperling (*Passer domesticus* L.). *Z. Vergl. Physiol.* **71**, 382–454.

Bryant, D. M. (1983). Heat stress in tropical birds: behavioural thermoregulation during flight. *Ibis* **125**, 313–323.

Buchholz, R. (1996). Thermoregulatory role of the unfeathered head and neck in male wild turkeys. *Auk* **113**, 310–318.

Butler, P. J., West, N. H. and Jones, D. R. (1977). Respiratory and cardiovascular responses of the pigeon to sustained level flight in a wind-tunnel. *J. Exp. Biol.* **71**, 7–26.

Byman, D., Wasserman, F. E., Schlinger, B. A., Battista, S. P. and Kunz, T. H. (1985). Thermoregulation of budgerigars exposed to microwaves (2.45 GHz, CW) during flight. *Physiol. Zool.* **58**, 91–104.

Carmi, N., Pinshow, B., Porter, W. P. and Jaeger, J. (1992). Water and energy limitations on flight duration in small migrating birds. *Auk* **109**, 268–276.

Chai, P. and Dudley, R. (1995). Limits to vertebrate locomotor energetics suggested by hummingbirds hovering in heliox. *Nature* **377**, 722–725.

Clark, J. A. (1976). Effects of surface emissivity and viewing angle on errors in thermography. *Acta Thermographica* **1**, 138–141.

Cossins, A. R. and Bowler, K. (1987). *Temperature Biology of Animals*. London: Chapman & Hall.

Craig, A. and Larochelle, J. (1991). The cooling power of pigeon wings. *J. Exp. Biol.* **155**, 193–202.

Dial, K. P., Biewener, A. A., Tobalske, B. W. and Warrick, D. R. (1997). Mechanical power output of bird flight. *Nature* **390**, 67–70.

Drent, R. H. and Stonehouse, B. (1971). Thermoregulatory responses of the Peruvian penguin, *Spheiscus humboldti*. *Comp. Biochem. Physiol.* **40**A, 689–710.

Gates, D. M. (1980). *Biophysical Ecology*. New York: Springer-Verlag.

Gubareff, G. G., Jansen, J. E. and Torborg, R. H. (1960). *Thermal Radiation Properties Survey*. Minnesota: Honeywell Research Center.

Hill, A. V. (1938). The heat of shortening and the dynamic constants of muscle. *Proc. R. Soc. Lond. B* **126**, 136–195.

Hill, R., Beaver, D. L. and Veghte, J. H. (1980). Body surface temperatures and thermoregulation in the black-capped chickadee (*Parus atricapillus*). *Physiol. Zool.* **53**, 305–321.

Hill, R. and Veghte, J. H. (1976). Jackrabbit ears: surface temperatures and vascular responses. *Science* **194**, 426–438.

Hirth, K.-D., Beisel, W. and Nachtigall, W. (1987). Pigeon flight in a wind tunnel. III. Regulation of body temperature. *J. Comp. Physiol.* B **157**, 111–116.

Holman, J. P. (1986). *Heat Transfer*. New York: McGraw Hill.

Incropera, F. P. and DeWitt, D. P. (1996). *Fundamentals of Heat and Mass Transfer*. New York: Wiley.

Kahl, M. P. (1963). Thermoregulation in the wood stork, with special reference to the role of the legs. *Physiol. Zool.* **36**, 141–151.

Klassen, M. (1995). Water and energy limitations on flight range. *Auk* **122**, 260–262.

Klir, J. J. and Heath, J. E. (1992). An infrared thermographic study of surface temperature in relation to external thermal stress in three species of foxes: the red fox (*Vulpes vulpes*), Arctic fox (*Alopex lagopus*) and kit fox (*Vulpes macrotis*). *Physiol. Zool.* **65**, 1011–1021.

Krattenmacher, R. and Rübsamen, K. (1987). Thermoregulatory significance of non-evaporative heat loss from the tail of the coypu (*Myocastor coypus*) and the tammar-wallaby (*Macropus eugenii*). *J. Therm. Biol.* **12**, 15–18.

Lancaster, W. C., Thomson, S. C. and Speakman, J. R. (1997). Wing temperature in flying bats measured by infrared thermography. *J. Therm. Biol.* **22**, 109–116.

Martineau, L. and Larochelle, J. (1988). The cooling power of pigeon legs. *J. Exp. Biol.* **136**, 193–208.

Masman, D. and Klassen, M. (1987). Energy expenditure during free flight in trained and free living Eurasian kestrels *Falco tinnunclus. Auk* **104**, 603–616.

McCafferty, D. J., Moncrieff, J. B., Taylor, I. R. and Boddie, G. F. (1998). The use of IR thermography to measure the radiative temperature and heat loss of a barn owl (*Tyto alba*). *J. Therm. Biol.* **23**, 311–318.

Möller, U. (1998). Aspekte der Flugkinematik des (Gemeinen) Stars (*Sturnus vulgaris*) beim Windkanalflug mit und ohne respiratorischer Maske. Diplomarbeit an der MatNatFak, Universität des Saarlandes.

Möller, U., Ward, S., Bilo, D., Speakman, J. R., Rayner, J. M. V. and Nachtigall, W. (1997). Effects of a respirometry mask on the mechanics of starling flight in a wind tunnel. *J. Morph.* **232**, 296.

Nachtigall, W. (1997). Methoden und Techniken zur bewegungsanalyse – schwimmende und fliegende Tiere. In *BIONA Report 11* (ed. A. Wisser, D. Bilo, A. Kesel and B. Möhl), pp. 1–56. Stuttgart: Gustav Fischer Verlag.

Norberg, U. M., Kunz, T. H., Steffensen, J. F., Winter, Y. and von Helversen, O. (1993). The cost of hovering and forward flight in a nectar-feeding bat, *Glossophaga sorcina*, estimated from aerodynamic theory. *J. Exp. Biol.* **182**, 207–227.

Phillips, P. K. and Sanborn, A. F. (1994). An infrared thermographic study of surface temperature in three ratites: ostrich, emu and double-wattled cassowary. *J. Therm. Biol.* **19**, 423–430.

Porter, W. and Gates, D. G. (1969). Thermodynamic equilibria of animals with environment. *Ecol. Monogr.* **39**, 227–244.

Price, J., Droege, S. and Price, A. (1995). *The Summer Atlas of North American Birds*. London: Academic Press.

Rayner, J. M. V. (1990). The mechanics of flight and bird migration. In *Bird Migration* (ed. E. Gwinner), pp. 283–299. Berlin: Springer-Verlag.

Rayner, J. M. V. (1995). Flight mechanics and constraints on flight performance. *Isr. J. Zool.* **41**, 321–342.

Ryan, B. F., Joiner, B. L. and Ryan, T. A. (1985). *The Minitab Handbook*. Boston: PWS-Kent.

Schmidt-Nielsen, K. (1984). *Scaling. Why is Animal Size so Important?* Cambridge: Cambridge University Press.

Sparrow, E. M. and Cess, R. D. (1966). *Radiation Heat Transfer*. Belmont: Brooks Cole Publishing.

Speakman, J. R., Hays, G. C. and Webb, P. I. (1994). Is hyperthermia a constraint on the diurnal activity of bats? *J. Theor. Biol.* **171**, 325–341.

Speakman, J. R. and Ward, S. (1998). Infrared thermography: principles and applications. *Zoology – Analysis of Complex Systems* **101**, 224–232.

Speakman, J. R., Ward, S., Möller, U., Jackson, D., Rayner, J. M. V. and Nachtigall, W. (1997). Thermography: a novel method for measuring the energy cost of flight? *J. Morph.* **232**, 326.

St-Laurent, R. and Larochelle, J. (1994). The cooling power of the pigeon head. *J. Exp. Biol.* **194**, 329–339.

Steen, I. and Steen, J. B. (1965). The importance of the legs in the thermoregulation of birds. *Acta Physiol. Scand.* **63**, 285–291.

Steketee, J. (1973). Spectral emissivity of skin and pericardium. *Phys. Med. Biol.* **18**, 686–694.

Thomas, A. L. R. (1996a). The flight of birds that have wings and a tail: variable geometry expands the envelope of flight performance. *J. Theor. Biol.* **183**, 237–245.

Thomas, A. L. R. (1996b). Why do birds have tails? The tail as a drag reducing flap and trim control. *J. Theor. Biol.* **183**, 247–253.

Tobalske, B. W. (1995). Neuromuscular control and kinematics of intermittent flight in the European starling (*Sturnus vulgaris*). *J. Exp. Biol.* **198**, 1259–1273.

Tobalske, B. W. and Dial, K. P. (1996). Flight kinematics of black-billed magpies and pigeons over a wide range of speeds. *J. Exp. Biol.* **199**, 263–280.

Torre-Bueno, J. R. (1976). Temperature regulation and heat dissipation during flight in birds. *J. Exp. Biol.* **65**, 471–482.

Torre-Bueno, J. R. (1978). Evaporative cooling and water balance during flight in birds. *J. Exp. Biol.* **75**, 231–236.

Tucker, V. A. (1968). Respiratory exchange and evaporative water loss in the flying budgerigar. *J. Exp. Biol.* **48**, 67–87.

Walsberg, G. E. (1988). Heat flow through avian plumages: the relative importance of conduction, convection and radiation. *J. Therm. Biol.* **13**, 89–92.

Ward, S., Möller, U., Rayner, J. M. V., Jackson, D. M., Nachtigall, W. and Speakman, J. R. (1998). Power requirement by starlings during wind tunnel flight. *Biol. Cons. Fauna*, **102** (in press).

Wathen, P. M., Mitchell, J. W. and Porter, W. P. (1974). Heat transfer form animal appendage shapes – cylinders, arcs and cones. *J. Heat Transfer, Trans ASME* **90**, 536–540.

Williams, T. M. (1990). Heat transfer in elephants: thermal partitioning based on skin temperature profiles *J. Zool., Lond.* **222**, 235–245.

Winter, Y. and von Helversen, O. (1998). The energy cost of flight: do small bats fly more cheaply than birds? *J. Comp. Physiol.* B **168**, 105–111.